

## The behaviour and evolution of fast oxygen ions injected into the TJ-II stellarator during neutral beam heating

K. J. McCarthy, J. Arévalo, V. Tribaldos, J.M. Fontdecaba, and TJ-II team

*Laboratorio Nacional de Fusión, Asociación EURATOM-CIEMAT, E-28040 Madrid, Spain*

<sup>2</sup>*Physics Department, Universidad Carlos III de Madrid, Leganés, Madrid, Spain*

### Introduction

The TJ-II is a 4-period heliac-type stellarator with a major radius of 1.5 m, a bean shaped plasma cross-section, with an average minor radius of  $\leq 0.22$  m, and magnetic field  $B(0) \leq 1$  T. It is designed to explore a wide rotational transform range ( $0.9 \leq \iota(0)/2\pi \leq 2.2$ ) in low, negative shear configurations ( $\Delta\iota/\iota < 6\%$ ) [1]. Plasmas, created with hydrogen, are heated using 2 gyrotrons operated at 53.2 GHz, the 2<sup>nd</sup> harmonic of the electron cyclotron resonance frequency ( $P_{ECRH} \leq 600$  kW,  $t \leq 300$  ms), and central electron densities,  $n_e(0)$ , and temperatures,  $T_e(0)$ , up to  $1.7 \times 10^{19}$  m<sup>-3</sup> and 2 keV, are attained. The TJ-II is the first heliac device to employ neutral beams for additional heating. At present, two injectors (NBI's) are operated and provide up to  $\sim 1$  MW ( $E_b \leq 32$  keV) for  $\leq 100$  ms. As a result plasmas with  $n_e(0) \leq 5 \times 10^{19}$  m<sup>-3</sup> have been attained. This heating system is comprised of two tangential injectors in the 'Co'-'Counter' configuration [2]. See Fig. 1. Each consists of an arc discharge source, acceleration grids, a neutralization chamber and ion dump. The cold dense plasma generated in the anodes ( $\sim 10^{14}$  H<sub>2</sub> cm<sup>-3</sup>,  $T_e = 5$  eV) is composed principally of H<sup>+</sup> and electrons with a not insignificant presence of molecular ions, *i.e.* H<sub>2</sub><sup>+</sup>, H<sub>3</sub><sup>+</sup>. However, impurities are also present in the source, *e.g.* accelerated impurities ions (*e.g.* H<sub>2</sub>O<sup>+</sup>, H<sub>3</sub>O<sup>+</sup>) undergo the same accelerating, disassociation and neutralization processes so their neutral particles exit with energies  $mE_b/M$  where m and M are the atomic masses of the resulting neutral particles and original impurity ions, respectively. Indeed, a low energy component is observed among the Doppler shifted H<sub>α</sub> spectral lines from TJ-II neutral beams. See Fig. 3 of Ref. [3]. Finally, all accelerated neutrals penetrate into the hot plasmas where they can be ionized, in collisions with protons and impurity ions, become trapped and travel around device.

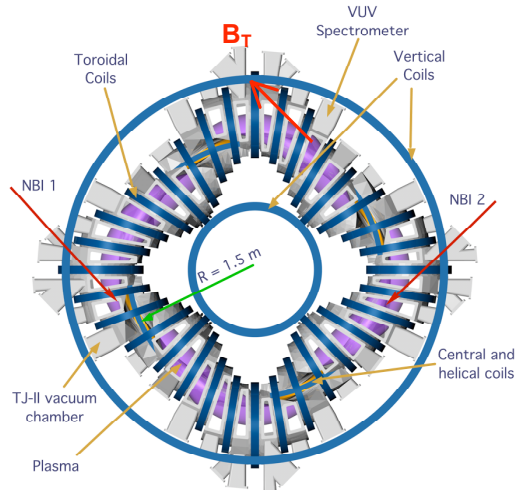


Fig. 1: Bird's eye view of the TJ-II

The TJ-II is equipped with numerous modern diagnostics including a VUV spectrometer. Time resolved emission line spectra are collected (in survey mode) every 5 ms using an f/10.4 1 m normal-incidence VUV spectrometer which is mounted with its wavelength dispersion plane perpendicular to the central conductor and located in a sector where its line-of-sight does not intercept either NBI beam path. See Fig. 1. Moreover, because of helicity, the angles  $\gamma$  between the line-of-sight and magnetic field line vectors are  $<90^\circ$ , *e.g.*  $\gamma \sim 55^\circ$  for the standard magnetic configuration, so spectral lines are shifted by poloidal and toroidal velocity components. For this work the viewing solid angle was restricted by stops to collect radiation from 10 cm of the plasma cross-section (about the central magnetic axis) plus a few centimetres in the toroidal direction.

### Observed Spectral Features during NBI heating

Broad line-like spectral features were observed about strong O III, O IV, O V and O VI lines during NBI heating in [3]. Indeed, their intensities can be  $\leq 20\%$  that of the main peak while their full-widths at half-maximum (FWHM),  $\sim 0.065$  nm, are significantly higher than would be expected for impurity temperatures typically measured in TJ-II, *i.e.* 50 to 200 eV [4]. Moreover, when NBI#1 is operated, the features appear on the short wavelength side of the lines, whilst when NBI#2 is operated, the features appear on their long wavelength side. Finally, when both NBI's are operated these features are present on both sides of the line (albeit asymmetrically), and disappear a few milliseconds after NBI switch-off. However, features are not observed about spectral lines from higher ionization states of oxygen, for instance about O VII lines about 162.3 nm nor about transitions of O VIII at 29.28 nm and 63.265 nm, respectively, all of which are tenuous or not observed in TJ-II plasmas.

As discussed in [3] the origin is O neutrals, from  $\text{H}_2\text{O}^+/\text{H}_3\text{O}^+$  ions accelerated to 30 kV in the ion source, that enter the plasma with velocity,  $V = 1.4 \times 10^3 (E_b/m)^{0.5} \text{ m s}^{-1}$ , are ionized, trapped and travel on a passing trajectory. The velocity of the trapped  $\text{O}^+$  becomes modified after ionization to  $V^2 = V_{\text{per}}^2 + V_{\text{par}}^2$ , ( $E_b = 1/2 m V_{\text{par}}^2 + \mu B_T$  and  $\mu = m V_{\text{per}}^2 / 2|B_T|$ ) where  $V_{\text{per}}$  and  $V_{\text{par}}$ , the velocities parallel and perpendicular to the toroidal magnetic field,  $B_T$ , depend on the angle  $\gamma$  between the vectors of  $B_T$  and  $V$  at the ionization point. Since injection is

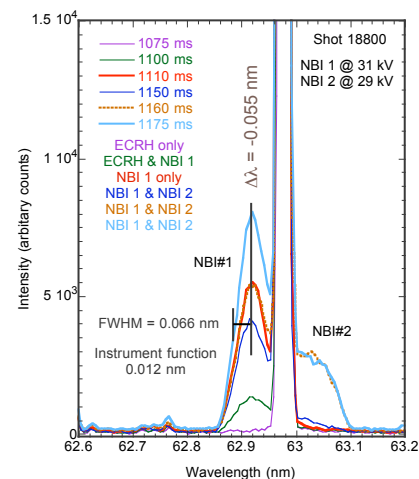


Fig 2: Features appear on the short and long wavelength sides of the O V line at 62.97 nm during NBI heating

tangential and ionization is highest in the plasma core ( $\rho < 0.6$ ),  $\gamma$  is typically  $\leq 15^\circ$  for the standard TJ-II configuration, 100\_44\_64, where the nomenclature reflects currents in the central, helical and vertical field coils, respectively. Then, each  $O^{+q}$  is ionized several times as it follows the magnetic field lines (in a cork screw manner) around the TJ-II before slowing down, (see table where  $\tau_{II} \gg \tau_{ion}$  when  $q < +6$ ), thus a Doppler displaced emission is observed from each ionization state that passes the spectrometer sector C6. Note the path lengths from NBI 1 to C6 ( $L_{1C6} = 6.7$  m) and from NBI 2 to C6 ( $L_{2C6} = 8.5$  m),  $V_{par} = 5.57 \times 10^5$  m<sup>-1</sup> for  $E_b = 30$  kV, and excitation is local (all  $A_{ki} > 10^8$  s<sup>-1</sup>).

The ‘critical’ beam energy,  $E_c$ , for fast  $O^{+1}$  ions during the initial NBI heated plasma phase is estimated as  $\sim 224$  keV (for  $T_e = 1$  keV) [5]. Moreover, as these ions become multiply ionized slowing down becomes exclusively due to collisions with protons ( $E_c \propto q^{2/3}$ ) and there is little or no pitch-angle scattering. The velocity slowing down time,  $\tau_{II}$ , is estimated as  $4\pi\epsilon_0^2 m V^2 / \Sigma_* n_* q_*^2 q_*^2 L / m_r$  where  $L$  and  $m_r$  are Coulomb logarithm and reduced mass, and \* represents background particles. In Table I,  $\tau_{II} \gg \tau_{ion}$  for each ionization state up to  $O^{+6}$ , thus ions are ionized before slowing and their spectral emission features reflect the parallel and perpendicular motions of the  $O^{+1}$  ions when created. Only for highly ionized states does  $\tau_{II} \approx \tau_{ion}$  and a slowing down spectrum is predicted. However, it has not been possible to verify this at present due to the weakness of O VII and O VIII lines in TJ-II. However, if electron temperature,  $T_e$ , falls below 100 eV, *e.g.* if density rises uncontrolled during NBI heating, then  $E_c$  approaches  $E_b$  and collisions with electrons become important. For such conditions  $\tau_{II}$  becomes comparable with  $\tau_{ion}$  and slowing down can be observed as a feature skewed towards the main unshifted spectral line. See Fig. 3.

It is has been found that the Doppler shift, given by  $(+/-) \lambda_0 V_{par} \cos \psi / c$ , where  $c$  is speed of light,  $\lambda_0$  is rest wavelength,  $\psi$  is as defined before, of the features is insensitive to magnetic configuration, *i.e.* to changes in  $\iota(0)$ , plasma volume and minor radius, for a range of configurations studied. However, the ratio of the intensities due to NBI# 1 and #2, ( $I_{nbi\#1} : I_{nbi\#2}$ ) may be sensitive to magnetic configuration but a more systematic study is needed to confirm this. It is also found that the fast  $O^{+q}$  structures require several milliseconds to build up after

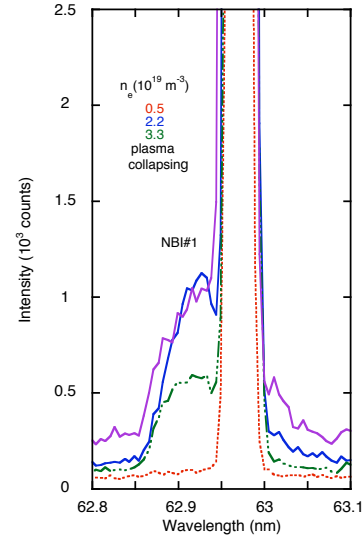


Fig. 3. Time evolution of the NBI #1 O V feature showing evidence for slow down of fast  $O^{+4}$  at plasma collapse: NBI#1 off, NBI #1 on, NBI #1 on, and plasma collapsing.

initial NBI current switch-on. Moreover the feature shape is initially skewed towards the main oxygen spectral line. Thereafter feature spectral shape and central wavelength remain unchanged as plasma density builds up during NBI injection. However the feature intensity does not vary directly with plasma density, rather it is dependent on several parameters, *i.e.* the neutral oxygen ionization rate, the density and  $T_e$  [via the collisional excitation rate,  $Q_e$ , as  $T_e^{-0.5} \exp(cT_e^{-1})$ , and fast oxygen ionization rates,  $Q_i$ , as  $T_e^{0.5} \exp(cT_e^{-1}) 1 - \exp(cT_e^{-1})$ ]. See Fig. 4. Finally, after NBI current switch-off the intensity of the fast  $O^{+q}$  spectral features decay within 1 or 2 ms.

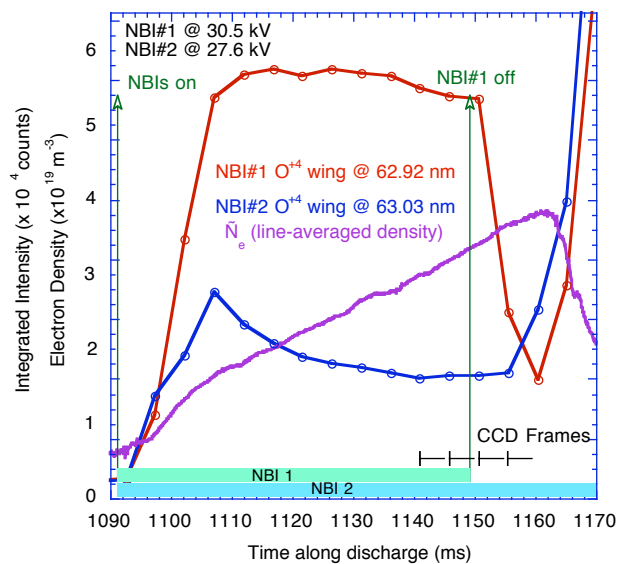


Fig. 4. Example of the evolution of O VI spectral features along an NBI heated TJ-II discharge.

$T_e^{-0.5} \exp(cT_e^{-1})$ , and fast oxygen ionization rates,  $Q_i$ , as  $T_e^{0.5} \exp(cT_e^{-1}) 1 - \exp(cT_e^{-1})$ ]. See Fig. 4. Finally, after NBI current switch-off the intensity of the fast  $O^{+q}$  spectral features decay within 1 or 2 ms.

|          | $\tau_{ion}(\mu s)$ | $\tau_{ion}(\mu s)$ | $l_{ion}(m)$ | $l_{ion}(m)$ | $\tau_{  }(ms)$ | $\tau_{  }(ms)$ |
|----------|---------------------|---------------------|--------------|--------------|-----------------|-----------------|
| Ion      | (a)                 | (b)                 | (a)          | (b)          | (a)             | (b)             |
| $O^{+1}$ | 3                   | 0.67                | 1.7          | 0.4          | 89              | 17              |
| $O^{+2}$ | 6                   | 1.3                 | 3.5          | 0.8          | 22.7            | 4.3             |
| $O^{+3}$ | 14.5                | 3.2                 | 8.4          | 1.9          | 10              | 2               |
| $O^{+4}$ | 31.7                | 7                   | 18.3         | 4.1          | 5.7             | 1               |
| $O^{+5}$ | 100                 | 22.2                | 60           | 13.3         | 3.6             | 0.67            |
| $O^{+6}$ | 2400                | 500                 | $>10^3$      | 300          | 2.5             | 0.47            |

Table: Ionization times,  $\tau_{ion}$ , ionization path lengths,  $l_{ion}$ , and slowing-down times,  $\tau_{||}$ , of ionization states of 30 keV oxygen neutrals injected into TJ-II for two plasma conditions, (a)  $\langle n_e \rangle = 10^{19} m^{-3}$ ,  $T_e(0) = 1$  keV,  $\langle n_i \rangle = 8 \times 10^{18} m^{-3}$ ,  $T_i = 70$  eV,  $L = 17.9$ , (b)  $\langle n_e \rangle = 3.5 \times 10^{19} m^{-3}$ ,  $T_e(0) = 300$  eV,  $\langle n_i \rangle = 3 \times 10^{19} m^{-3}$ ,  $T_i = 110$  eV,  $L = 17$ .

### Acknowledgements

This work is partially financed by the Spanish *Ministerio de Ciencia e Innovación*, Ref. FTN2007-64159.

### References

- [1] C. Hidalgo *et al.*, Nucl. Fusion, 45 (2005), S266.
- [2] M. Liniers *et al.*, Vacuum 67 (2002) 379.
- [3] K. J. McCarthy *et al.*, to appear in J. Phys. B. At. Mol. Opt. Phys. (2010).
- [4] J. M. Carmona *et al.*, Fusion Sci. Tech. 54, (2008) 962.
- [5] R. J. Goldston and P. H. Rutherford, *Introduction to plasma physics*, Institute of Physics Publishing, Bristol and Philadelphia (1995).